Atmospheric
Measurement
Techniques
Open Access
Discussions

AMTD

7, 3953–3991, 2014

Validation of MIPAS IMK/IAA V5R_O3_224 ozone profiles

A. Laeng et al.

Title Page

Abstract | Introduction

Conclusions | References

Tables | Figures

|◄ | ►|

◄ | ►

Back | Close

Full Screen / Esc

Printer-friendly Version

Interactive Discussion

Validation of MIPAS IMK/IAA V5R_O3_224 ozone profiles

A. Laeng[1], U. Grabowski[1], T. von Clarmann[1], G. Stiller[1], N. Glatthor[1],
M. Höpfner[1], S. Kellmann[1], M. Kiefer[1], A. Linden[1], S. Lossow[1], V. Sofieva[6],
I. Petropavlovskikh[15], D. Hubert[16], T. Bathgate[9], P. Bernath[19], C. D. Boone[5],
C. Clerbaux[8], P. Coheur[2], R. Damadeo[7], D. Degenstein[9], S. Frith[10],
L. Froidevaux[4], J. Gille[11], K. Hoppel[18], M. McHugh[2], Y. Kasai[12], J. Lumpe[17],
N. Rapoe[3], G. Toon[4], T. Sano[13], M. Suzuki[13], J. Tamminen[6], J. Urban[14],
K. Walker[5], M. Weber[3], and J. Zawodny[7]

[1]Institut für Meteorologie und Klimaforschung, Karlsruhe Institute of Technology, Karlsruhe, Germany
[2]ULB, Brussels, Belgium
[3]Institut für Umweltphysik, University of Bremen, Bremen, Germany
[4]Jet Propulsion Laboratory, California Institute of Technology, Pasadena, CA 91109, USA
[5]University of Toronto, Toronto, Canada
[6]Finnish Meteorological Institute, Helsinki, Finland
[7]NASA Langley Research Center, Hampton, USA
[8]Sorbonne Université, UPMC Univ. Paris 06, Université Versailles St-Quentin, CNRS/INSU, LATMOS-IPSL, France and ULB, Brussels, Belgium

[9]University of Saskatchevan, Saskatoon, Saskatchewan, Canada
[10]Science Systems and Applications Inc., Lanham, MD, USA
[11]University of Colorado, Boulder, CO, USA
[12]NICT, Koganei, Tokyo, Japan
[13]JAXA, Tsukuba, Japan
[14]University of Chalmers, Göteborg, Sweden
[15]NOAA, Boulder, CO, USA
[16]BIRA, Brussels, Belgium
[17]Computational Physics, Inc., Boulder, CO, USA
[18]Naval Research Laboratory, Washington DC, USA
[19]Old Dominion University, Norfolk, VA, USA

Correspondence to: A. Laeng (alexandra.laeng@kit.edu)

Title Page

Abstract | Introduction

Conclusions | References

Tables | Figures

|◄ | ►|

◄ | ►

Back | Close

Full Screen / Esc

Printer-friendly Version

Interactive Discussion

Abstract

We present the results of an extensive validation program of the most recent version of ozone vertical profiles retrieved with the IMK/IAA MIPAS research level 2 processor from version 5 spectral Level 1 data. The time period covered corresponds to
5 the reduced spectral resolution period of the MIPAS instrument, i.e. January 2005–April 2012. The comparison with satellite instruments includes all post-2005 satellite limb and occultation sensors having measured the vertical profiles of tropospheric and stratospheric ozone: ACE-FTS, GOMOS, HALOE, HIRDLS, MLS, OSIRIS, POAM, SAGE II, SCIAMACHY, SMILES, and SMR. In addition, balloon-borne MkIV solar occul-
10 tation measurements and groundbased Umkehr measurements have been included, as well as two nadir sensors: IASI and SBUV. For each reference dataset, bias determination and precision assessment are performed.

Better agreement with reference instruments than for the previous data version, V5R_O3_220 (Laeng et al., 2013), is found: the known high bias around the ozone vmr
15 peak is significantly reduced and the vertical resolution at 35 km has been improved.

The agreement with limb and solar occultation reference instruments that have a known small bias vs. ozone sondes is within 7 % in the lower and middle stratosphere and 5 % in the upper troposphere. Around the ozone vmr peak, the agreement with most of satellite reference instruments is within 5 %; this bias is as low as 3 % for
20 ACE-FTS, MLS, OSIRIS, POAM and SBUV.

1 Introduction

In order to improve the predictive quality of atmospheric models, their constraints must be well refined. For this, the atmospheric processes underlying the fluctuation of the budget of atmospheric constituents should be understood well enough. For instance,
25 despite expectations for a slow recovery of the stratospheric ozone layer in the coming decades, record or very low temperatures occurred in 2006 and 2011, leading to some

Validation of MIPAS IMK/IAA V5R_O3_224 ozone profiles

A. Laeng et al.

of the deepest ozone holes over Antarctica. Understanding such ozone fluctuations Understanding such ozone fluctuations is impossible without well-resolved high-quality measurements of vertical profiles of this important stratospheric gas. The pole-to-pole day-and-night measurements of ozone provided by the MIPAS instrument in 2002–
5 2012 represent an important dataset for this purpose.

MIPAS is an instrument that was carried on the European ENVISAT satellite; along with ∼ 30 other atmospheric trace gases, MIPAS measured vertical profiles of ozone. MIPAS measured day and night, pole-to-pole, providing more than 1300 profiles per day. The failure of a MIPAS mirror slide in 2004 led to the division of the 10 years of
10 MIPAS data into two operational periods: 2002–2004 when the instrument measured with high spectral resolution (usually referred to as "full-resolution (FR) period") and 2005–2012 when instrument measured with lower spectral but better vertical resolution ("reduced resolution (RR) period"). The MIPAS data from these two periods are evaluated separately.
15 In this paper we present the results of an extensive validation of vertical ozone profiles retrieved from MIPAS reduced resolution spectra with the IMK/IAA research processor. The MIPAS IMK/IAA dataset has been used as part of the SPARC Data Initiative (Tegtmeier et al., 2013) and in the HARMOZ databank (Sofieva et al., 2013). The ozone dataset from MIPAS IMK/IAA processor was selected to be used in the framework of the
20 European Ozone Climate Change Initiative Project, after an extensive Round Robin intercomparison of four existing MIPAS processors: the ESA operational processor with the scientific prototype hosted at IFAC Florence (Raspollini et al., 2013), a research processor hosted at ISAC Bologna (Carlotti et al., 2001, 2006), a research processor hosted at the University of Oxford (http://www.atm.ox.ac.uk/MORSE/), and the IMK/IAA
25 processor. See Laeng et al. (2013) for a homogenized description of the four MIPAS processors and for details of the analysis performed. In the rest of this paper, "MIPAS dataset" will refer to the MIPAS IMK/IAA dataset.

Title Page

Abstract | Introduction

Conclusions | References

Tables | Figures

◄ | ►

◄ | ►

Back | Close

Full Screen / Esc

Printer-friendly Version

Interactive Discussion

2 MIPAS IMK/IAA V5R_O3_224 profiles

The description of the processing scheme of MIPAS IMK/IAA research processor and its adaptation to the Reduced Resolution spectra of MIPAS are published in von Clarmann et al. (2003) and von Clarmann et al. (2009). As shown in Laeng et al. (2013), all four MIPAS processors have a high bias around the ozone vmr peak (approximatively 35 km) compared to ozonesondes, lidars, ACE-FTS and MLS. Though the IMK/IAA Processor had the smallest bias, ozone mixing ratios were still higher by up to 0.2 ppmv than those of MLS. In addition, the ozone from the MIPAS IMK/IAA Processor (labeled in Laeng et al., 2013 as "KIT processor") had a peak of particularly poor vertical resolution at 35 km and the position of the ozone vmr peak was slightly higher than in the reference instruments, causing the high bias around the ozone vmr maximum.

The version of ozone profiles used in the analysis by Laeng et al. (2013) was V5R_O3_220. In the production of this version, the microwindows from both MIPAS band A (685–970 cm^{-1}) and band AB (1020–1170 cm^{-1}) were used. The displaced ozone vmr maximum as well as the peak in vertical resolution were both appearing at heights where the microwindows from the AB band were activated. It was pointed out already in Glatthor et al. (2006) that the exclusive use of band A microwindows can lower the ozone values at heights corresponding to the ozone vmr maximum. The reason for this is possibly an inconsistency among the spectroscopic data for the ozone bands located in MIPAS band A vs. band AB. Hence, in order to minimize the high bias, a new version of ozone was produced, namely version V5R_O3_224.

The differences with respect to the version V5R_O3_220 used in the Round Robin exercise are the following:

– No microwindows from the band AB were used at heights below 50 km; this reduced the bias around the ozone vmr maximum and fixed the problem of the displacement of the ozone vmr peak (see Fig. 1 for comparison of mean ozone profiles from the versions V5R_O3_220 and V5R_O3_224). As one can see in

Fig. 1, the values at the ozone vmr maximum of the version V5R_O3_224 are slightly larger than the values of V5R_O3_220. However, the bias of V5R_O3_224 around the ozone vmr maximum is still smaller than the bias for the three other MIPAS Processors: to demonstrate this, we overplotted the bias of V5R_O3_224 on the bias panel of comparison with MLS from Laeng et al. (2013), this is shown in Fig. 2.

– To compensate for the loss of information implied by dropping the AB microwindows at heights below 50 km, in this height range, three times more microwindows were used in the A band, see Table 1. This improved the previously poor vertical resolution around the ozone vmr maximum; Fig. 3 shows the vertical resolution of the previous version (left panel) and of the version under validation (right panel) for typical mid-latitude retrieval. The oscillating behaviour of the vertical resolution comes from the fact that the retrieval is performed on the grid finer than the original tangent height grid: the vertical resolution is better at gridpoints close to a tangent altitude of the measurement and worse between two adjacent tangent altitudes.

– The altitude-dependent strength of the regularization has been changed. The regularization matrix is now

$$\mathbf{L_1}^T \begin{pmatrix} \gamma_1 & \dots & 0 \\ & \ddots & \\ 0 & \dots & \gamma_n \end{pmatrix} \mathbf{L_1} + \mathbf{D} \tag{1}$$

where $\mathbf{L_1}$ is an $(n-1) \times n$ finite differences matrix, γ_i are the altitude-dependent regularization strengths, and $\mathbf{D}$ is a matrix which is zero except for the diagonal values referring to the uppermost altitudes, which ties ozone to values near zero there.

– The strength of the constraint, γ_i, was taken constant up to 70 km (in contrast to 65 km for the version V5R_O3_220)

3958

The data used in this paper come from two versions: V5R_O3_224 (2005–April 2011) and V5R_O3_225 (May 2011–April 2012). The difference between versions V5R_O3_224 and V5R_O3_225 is only marginal: for version V5R_O3_224 ECMWF temperature profiles which are used as a priori for temperature retrieval, were derived from the NILU data server, while for V5R_O3_225 the ECMWF temperatures directly from ECMWF were used, since NILU does not make ECMWF profiles available anymore. No relevant ozone differences were found in response to this change.

3 Overview of reference instruments

The reference datasets used in this study are summarized in Table 2. All spaceborne limb and occultation instruments that have flown and measured tropospheric/stratospheric ozone vertical profiles at the same time as MIPAS are included. We also include the comparison with two nadir sensors: IASI and SBUV, as well as with the vertical profiles from MkIV balloon measurements and Umkehr measurements. We do not include ozonesondes and lidars because extensive comparison with these was made in Laeng et al. (2013) for the previous version of the data. The IMK/IAA MIPAS ozone dataset was found to deviate by less than 5 % from ozonesondes (10 % for tropical regions), and Fig. 1 of this paper demonstrates that the previous version and the current version under validation are almost identical in the altitude range covered by ozonesondes.

4 Comparison methodology

For all satellite reference datasets except MLS, the optimal ratio (number of collocations)/(distance between measured air parcels) was achieved with the collocation criteria of 5 h and 500 km. For the dense sampling of MLS, the collocation criteria were tightened down to 4 h and 250 km. Note that the time interval of 4 h cannot be made shorter because it must be larger than the difference in equator

Validation of MIPAS IMK/IAA V5R_O3_224 ozone profiles

A. Laeng et al.

Title Page

Abstract | Introduction

Conclusions | References

Tables | Figures

◄ | ►

◄ | ►

Back | Close

Full Screen / Esc

Printer-friendly Version

Interactive Discussion

crossing local times of the carrying platforms (which are 10 a.m. for Envisat carrying MIPAS and 1.30 p.m. for Aura carrying MLS), otherwise the set of tropical collocations would be reduced. For MkIV and Umkehr datasets, the collocation criteria were taken 24 h and 1000 km.

Application of collocation criteria produced the set of matched pairs, reported in Table 2. All the plots in this study, including climatologies, were produced out of the collocated measurements. Figure 4 shows the latitudinal distributions over months of collocated measurements of MIPAS with each satellite reference instrument.

All reference datasets except Umkehr were interpolated onto the MIPAS retrieval grid, which is a fixed altitude grid with 1 km steps between 6 and 44 km and 2 km steps between 44 and 70 km. Datasets delivered on an altitude grid were interpolated linearly. As the MIPAS IMK/IAA processor has a reliable pressure–altitude relation (see Sect. 6.3.4 of Laeng et al., 2013), the datasets provided on a pressure grid were interpolated via pressure in logarithmic domain using MIPAS pressures. Datasets provided in number density units were also transformed into volume mixing ratio by using the temperatures from the MIPAS retrieval. For GOMOS, number density was converted into mixing ratio using ECMWF + MSIS90 air density profiles at occultation locations. The discrepancies between the vertical resolutions of limb and occultation reference datasets and vertical resolution of MIPAS do not exceed a factor 1.5–2. For these datasets, sensitivity tests were performed and showed that within these margins, the application of averaging kernels is not relevant. Hence, no averaging kernels were applied when comparing with limb and occultation datasets. Nadir sensors have vertical resolution which are quite different from MIPAS. When comparing with IASI, MIPAS dataset was convolved with IASI genuine averaging kernels. At the time when the analysis described in this paper was perfomed, no averaging kernels for individual SBUV ozone profiles were available, hence the comparison with SBUV was performed without taking into account the discrepancies in vertical resolutions. For the comparison with Umkehr, the MIPAS dataset was transformed into Dobson Units (DU) on Umkehr layers, the details are described in Sect. 6.

To assess the bias between MIPAS and a reference instrument, we calculate the mean difference on n collocated pairs

$$\text{MD} = \frac{1}{n} \sum_{i=1}^{n} (x_{i,\text{MIPAS}} - x_{i,\text{ref}}) \tag{2}$$

or, in short notation (MIPAS – REF). The percentage bias with respect to a reference instrument is calculated as follows:

$$\text{bias} = 100\,\% \times \frac{\text{MIPAS} - \text{REF}}{\text{REF}}. \tag{3}$$

One could argue that the normalization should be taken the same for all instruments, in other words, the denominator in the last equation should be MIPAS. It is however our choice to show the biases with respect to reference instruments, in order to obtain independent estimates of the bias. This of course implies that the biases with respect to different reference instruments calculated in this way can not be directly compared to each other, except if the reference instruments have very similar mean profiles.

An assessment of precision is performed by analysis the residual variance of MIPAS dataset with respect to reference datasets, namely by comparing the standard deviation of differences

$$\text{STOD} = \sqrt{\frac{1}{n-1} \sum_{i=1}^{n} ((x_{i,\text{MIPAS}} - x_{i,\text{ref}}) - \text{MD})^2} \tag{4}$$

with the combined error

$$\text{CE} = \sqrt{(\text{mean MIPAS error})^2 + (\text{mean ref. instr. error})^2} \tag{5}$$

calculated still on collocated profiles only, see von Clarmann (2006). Such analysis is partly impeded by the fact that not all reference instruments provide full random error

Title Page

Abstract | Introduction

Conclusions | References

Tables | Figures

|◄ | ►|

◄ | ►

Back | Close

Full Screen / Esc

Printer-friendly Version

Interactive Discussion

estimates (see last but one column in Table 2). Since for most reference instruments only measurement noise is reported, the estimated error of the differences between co-incident measurements is expected to be lower than the standard deviation of the differences. In addition, the latter quantity includes the natural variability of ozone within the given collocation criteria. Thus, only upper estimates on the reliability of the MIPAS precision from these reference measurements can be made. Laeng et al. (2013) presented an approach to precision validation of vertical ozone profiles by a method not involving any reference instrument, and concluded that MIPAS IMK/IAA precision estimates for ozone are close to reality.

5   Comparison with satellite measurements

Figures 5 and 6 present the estimated bias and precision assessment of MIPAS ozone profiles with respect to reference instruments. To avoid the overloading of the bias summary plots, the satellite reference datasets were subdivided into two classes according to their biases with respect to ozonesondes: those having a known small bias in the main ozone layer (20–30 km) and those having a slightly larger bias in the main ozone layer. For this purpose, for each dataset, the estimation of the bias with respect to ozonesondes was taken from the latest validation study performed on a dataset from the same instrument and processor. The latest validation studies of reference instruments and biases found in them are summarized in the last column of Table 2. We would like to point out that these bias estimates are in agreement with estimates obtained in Hubert et al. (2012, 2014) even though different versions of datasets were used in those studies.

The left panels of Figs. 5 and 6 represent the percentage bias with respect to the reference instruments. The curves on the right panels of Figs. 5 and 6 represent the residual variance which is calculated as the discrepancy between the standard deviation of

the differences and combined errors:

$$RV = 100\,\% \times \frac{\sqrt{STOD^2 - CE^2}}{MIPAS}. \tag{6}$$

This quantity estimates how large the relative natural variability must be to justify the observed spread, if the error estimates were realistic. The latter curves should be treated with caution and not be overinterpreted: even though by their definition these curves represent estimates of natural variability within the collocation window 5 h and 500 km, and provide an upper estimate on MIPAS random error, it must not be forgotten that for different reference instruments they are calculated on different matched pairs, that can have different latitudinal distributions. If a significant number of collocations with a dataset occur at higher latitudes in winter, where natural variability of ozone is big, the corresponding residual variance is expected to be elevated. This is for instance the case for comparisons with ACE-FTS, GOMOS, and POAM: a significant fraction of their collocations occur at higher latitudes in winter and spring (Fig. 4), and the corresponding residual variances on right panels on Figs. 5 and 6 are expectedly elevated.

For a dataset with relatively homogemious latitudinal distribution of collocations, anomalously large values of RV, or negative values of RV^2 would indicate that the error estimates of one or both instruments are non-realistic. For a number of instruments on Figs. 5 and 6 the residual variance at 25–45 km heights is about the same, with estimated number about 4 %. Assuming that MIPAS error estimates are realistic (Laeng et al., 2013), this hints that remaning instruments, having residual variance too large, have deficiencies in their error estimates.

One sees from Fig. 5 that for the main ozone layer (20–30 km), the bias of MIPAS with known small-biased datasets is within 7 %, while in the upper troposphere (15–20 km) and at 30–40 km heights the bias is within 5 %. Around the ozone vmr peak, the agreement with ACE-FTS, MLS and OSIRIS is within 3 %. The bias with respect to MLS is similar to the bias with respect to SAGE II in the main ozone layer: it is positive

and of order 4–5 %. Between 30 and 45 km, the bias with respect to MLS is of the same sign and magnitude, while the bias with respect to SAGE is twice as large. The smallest bias in Fig. 5 is observed vs. ACE: it remains within 2 % in the stratosphere and takes both signs. In turn, at 46–56 km heights, the bias with respect to ACE-FTS is the largest in absolute value on this panel: it is negative and reaches 15 %. Above 60 km, all reference instruments except SCIAMACHY demonstrate that MIPAS ozone is biased high. The best agreement above 60 km is observed with two other Envisat sensors: positive bias vs. GOMOS does not exceed 8–21 %, and bias vs. SCIAMACHY does not exceed 17 % when it is negative and does not exceed 22 % when it is positive at 69–70 km heights. MIPAS is biased high by 0 to 7 % vs. all instruments collected in Fig. 5 between 20 and 40 km altitude.

Figure 6 provides biases vs. instruments which are known to have larger (between 5–7 and 20 %) biases vs. ozone sondes. In general, the comparisons resemble those of the small-biased instruments: the biases are always positive for 25–40 km heights, except fot IASI, with values between 0 and +10 %. Below and above this height range, the spread among the instruments is larger and cover both positive and negative values between −20 and +20 %. The IASI bias in the UTLS is the largest on this panel, going up to 20 % in the main ozone layer. Such a bias of IASI at this altitude was already reported by e.g. Dufour et al. (2012). Above 30 km the sensitivity of IASI drops, as shown by the averaging kernels (Keim et al., 2009) and the profiles just reproduce the a priori.

The SMR dataset provides quite large error bars on the whole height range of ozone profiles, which leads to the large combined error that sometimes does exceed the standard deviation of differences. In this case the estimate of the square of the residual variability is negative, this is why there is no green SMR curve between 32 and 45 km heights.

A relatively small (within 4 % in the stratosphere) bias with respect to POAM (brown curves in Fig. 6) goes along with a large estimate of residual variability: the residual variability derived from MIPAS-POAM is three times as large as that derived from most

of other instruments. The reasons are two-fold: MIPAS-POAM coincidences occur high latitudes only (see POAM panel on Fig. 4), where geophysical variability tends to be higher relative to low latitude coincidences. Assuming that MIPAS error estimates are realistic, as suggested in Laeng et al. (2013), this big residual variance could also be an indication that the POAM uncertainties are underestimated. Similar conclusions can be drawn for IASI (yellow curve in Fig. 6).

Comparisons with HALOE, HIRDLS, SCIAMACHY and both SMILES processors all expose a similar behavior of MIPAS ozone data relative to these instruments: MIPAS is positively biased by less than 10 % in the stratosphere.

The SCIAMACHY curve is absent at most heights on the right panel of Fig. 6 because the combined error of SCIAMACHY-MIPAS comparison exceeds almost everywhere the standard deviation of differences which gives negative RV^2 quantity. This agrees with the conclusions of the analysis performed in the framework of Ozone_cci project: SCIAMACHY seems to overestimate its uncertainties up to a factor of 2.5 and MIPAS uncertainties estimates are roughly realistic.

The SBUV curve is absent on the right panel of Fig. 6 because the version 8.6 of SBUV data which is used for this analysis is provided without error estimates.

The behaviour of the bias around the ozone vmr maximum in the comparison with small-biased data sets shows a systematic high MIPAS bias at this height range (left panels of Figs. 5 and 6), while some of not-small (with respect to ozonesondes) biased data sets have zero bias with MIPAS, for instance SBUV, SCIAMACHY, SMILES_NICT and POAM. This observation should be taken into the context namely that the separation of reference instruments into "small-biased" and "not so small-biased" was done based on their comparison with ozonesondes, which do not go higher than 30 km. Compared to instruments with a known small bias vs. ozone sonde data, MIPAS is always biased high around the ozone vmr maximum (left panel of Fig. 5). In contrast, the MIPAS bias is smaller and sometimes even zero in comparison to the instruments which have a slightly larger bias vs. ozone sondes (see left panel of Fig. 6). The interesting point is that the comparison to ozonesondes which led to the binning into the

Validation of MIPAS IMK/IAA V5R_O3_224 ozone profiles

A. Laeng et al.

Title Page

Abstract | Introduction

Conclusions | References

Tables | Figures

|◀ | ▶|

◀ | ▶

Back | Close

Full Screen / Esc

Printer-friendly Version

Interactive Discussion

two instrument groups ends below the altitude of the ozone vmr maximum. This means that the behavior of the instruments with respect to ozone sondes can be extrapolated to larger altitudes. Further, all comparisons to satellite reference instruments reveal a local maximum of the bias around 44 km, independent of the sign of the bias in this altitude region. This hints towards an artefact in MIPAS data, visible as a small bulge in the profiles in Fig. 1. The reason for this artefact is still unidentified. For a large number of reference instruments, the natural variability within the collocation radius necessary to explain the scatter if the error estimates were realistic is only about 5 %, although some of the error estimates include only measurement noise. Thus, this defines an upper limit by which the MIPAS error can be underestimated. Finally, comparisons with seven datasets (MLS, SAGE, OSIRIS, as well as HALOE, HIRDLS and both SMILES datasets) agree on the estimates of about 4 % natural variability within 5 h and a 5 km collocation window between 23 and 48 km.

Figure 7 shows the scatter plots with small-biased solar occultation and limb mea-surements. The axes of this plot correspond to ozone volume mixing ratios derived from MIPAS and the reference instrument, and the color scale denotes the heights, as indicated at the right of the plot. In order to make all four plots comparable, we re-stricted height to the uppermost height of OSIRIS datapoints, 54 km. The size of the scatter around the straight line of unity slope going through the origin indicates that the noise in one or both data sets, and/or the amount of natural variability within the chosen colocation window is important. An offset from the ideal line hints at an addi-tive bias; a slope different from unity hints at a multiplicative bias, and a curved line is an indication of a nonlinear or altitude-dependent bias. For high ozone values, the distribution of data points is centered not exactly around the reference line, but shifted below which indicates the high bias of MIPAS ozone data near the ozone vmr maxi-mum. Data points below the reference line for high ozone values confirm the high bias of MIPAS ozone near the ozone maximum. The area above the reference line around 3.5 ppmv and 50 km (most obvious for the correlation with ACE-FTS) corresponds to the local low bias of MIPAS ozone which is clearly visible in Figs. 5 and 6. Except for

Validation of MIPAS IMK/IAA V5R_O3_224 ozone profiles

A. Laeng et al.

Title Page

Abstract | Introduction

Conclusions | References

Tables | Figures

◄ | ►►

◄ | ►

Back | Close

Full Screen / Esc

Printer-friendly Version

Interactive Discussion

these issues, the data points in the scatter plots are confined to a narrow band around the reference line in all cases. One notes in Fig. 7 that the width of the distribution of data points around the reference lines appears to be larger for MLS and OSIRIS than for ACE-FTS and SAGE. However, since the number of datapoints is much smaller for the latter than for the former, and because this representation is not normalized with respect to the number of datapoints, no conclusion on errors or variability can be drawn from this.

A comparison of the evolution of ozone distributions over height with time as measured by MIPAS and MLS is shown in Fig. 8. One observes that MLS (upper panel) and MIPAS (middle panel) see the same atmospheric variability, which in addition is consistent with seasonal cycle of monthly zonal mean ozone curves from climatology comparison of SPARC Data Initiative, c.f. Fig. 6 and left bottom panel of Fig. 8 in Tegtmeier et al. (2013). Clear seasonal cycle can be seen in the lower panel on Fig. 8, where the monthly means of percent differences of measurements for collocated pairs are shown. Note that this seasonal cycle is present in absolute as well as in relative differences with dense samplers MLS and OSIRIS (see Fig. 9). The reasons for this seasonality in the bias is currently under investigation: this could be due to a possibly multiplicative nature of the bias or to a time-dependence of the ozone vmr values themselves. It could also partly arise from tangent pressure and/or temperature systematic differences between measurements. Note that this seasonality of the bias does not affect the trend calculation from the paper by Eckert et al. (2014) because the seasonal cycle is fitted in their regression model.

Finally, five reference instruments presented here are used together with MIPAS IMK/IAA in the HARMOZ databank (Sofieva et al., 2013): ACE-FTS, GOMOS, OSIRIS, SCIAMACHY, and SMR. The bias with respect to these five datasets from HARMOZ agrees well with the analysis of the bias presented in Fig. 6 of Sofieva et al. (2013).

Title Page

Abstract | Introduction

Conclusions | References

Tables | Figures

◄◄ | ►►

◄ | ►

Back | Close

Full Screen / Esc

Printer-friendly Version

Interactive Discussion

6 Comparison with Umkehr measurements

Umkehr measurements are based on zenith sky observation of Solar radiation at two wavelengths in the UV part of the Solar spectrum. One wavelength is strongly absorbed by ozone and the other is not. Ratio is measured as function of SZA. From these observations the optimum statistical solution is found. The vertical resolution of Umkehr ozone profiles is derived from the analysis of the averaging kernel matrix where the full width at half-maximum (FWHM) is 5 km, taking into account that the bottom layers (pressure between surface and 250 hPa) is derived as double layer. The retrievals are done on days with clear sky conditions (clear zenith). The method was developed to minimize the a priori contribution on the retrieval (Petropavlovskikh et al., 2005). The dataset is also corrected for the stray light contribution, which reduces the typical offset of Umkehr profiles in the upper layers, making the dataset optimized for monthly means' calculation. Above 32 hPa the operational Umkehr retrieval is known to underestimate ozone by as much as 5–10 % when compared to the SBUV profiles (Kramarova et al., 2013). The problem is corrected in the dataset used in this analysis by including estimates of the stray light contributions to the observed Umkehr measurements.

For the sake of brevity, we show here the comparison only with data points from the Boulder station (40° N) where almost daily profiles from 2005 to 2012 have been taken with a Dobson instrument. The comparison with four stations at different latitudes can be found in Laeng and Petropavlovskikh (2013).

As Umkehr has a known bias on individual profile levels, but the current retrieval algorithm is optimized for monthly mean calculations, we first compare monthly mean values from both instruments. Left column of Fig. 10 shows the monthly mean ozone values (in DU) of Umkehr and MIPAS overpasses as function of time and atmosheric pressure in 2005–2012 at Boulder station (40° N, 105° W). The color code on the right side represents ozone (DU) in Umkehr layers (top pressure of the layer is half of the pressure at the bottom). The vertical axes are $\log_{10}$ (pressure). The right column of Fig. 10 represents the absolute and relative differences between Umkehr and

MIPAS profiles as function of time and pressure. The relative differences are mostly within ±10 %, with the exception of the layer between 32 and 16 hPa, where differences are larger (±20 %). The seasonal cycle in the absolute bias as observed in comparison with satellite instruments, can also be observed in the comparison of MIPAS with Umkehr at the Boulder station. But unlike in satellite case, this seasonal cycle is less pronounced in relative bias plots (see right column of Fig. 10). This hints that the bias vs. Umkher is dominated by its additive component. This seasonal cycle in the absolute bias is also well pronounced in the comparison with Syowa station situated at high southern latitude (−69° S) (Laeng and Petropavlovskikh, 2013). On the other hand, in comparisons at Lauder (−45° S) and Mauna Loa (19.5° N) stations, there is no clear indication of seasonality of absolute bias of MIPAS with respect to Umkehr (Laeng and Petropavlovskikh, 2013).

To evaluate the bias on individual profile level, distributions of individual MIPAS and Umkehr values in two Umkehr layers: layer 5 (appr. 1.5–1.2 on y axis) and layer 7 (appr. 0.9–0.5 on y axis) were compared (Fig. 11). The histograms have the same shapes and numbers of modes, but there is an offset in the position of the modes. MIPAS is systematically biased high with respect to the Umkehr measurements. Similar high and low biases of MIPAS in the relevant altitude ranges have not been found in comparisons with any satellite instruments (see Sect. 5). For this reason we tentatively assign the biases to the Umkehr measurements.

7 Comparison with MkIV balloon measurements

Figure 12 presents the comparison of MIPAS ozone measurements with the three MkIV balloon profiles (Toon, 1991) within the MIPAS reduced resolution period. The first two MkIV profiles, from 20 September 2005 and 22 September 2007, were measured when MIPAS was temporarily inactive and no matches were found within 24 h and 1000 km. All three flights for which the matches were found took place in September months. The

profiles were hence compared to September and seasonal (SON, September-October-November) means of MIPAS in [30° N; 40° N] latitudes.

For all three flights, no indication of a high MIPAS bias near the ozone vmr peak, which was oberved in the comparison with satellite instruments, is found: the seasonal means present lower than MkIV values, while the September means agree well with MkIV profiles over the entire altitude range. For the profile from sunrise of 23 September 2007, three collocated MIPAS profiles were found (green lines). For the closest of these 3 profiles, the maximum deviation from MkIV profiles is 0.3 ppmv and near the ozone vmr peak the agreement is excellent. It should be kept in mind though that is difficult to build enough statistics with a few balloon flights to get out a significant bias. Hence we can draw no conclusions regarding whether this bias corroborates or not the biases that were observed in satellite comparisons.

8 Conclusions

Ozone vertical profiles retrieved from MIPAS spectra with the IMK/IAA research processor, version V5R_O3_224, were compared with ozone vertical profiles from ACE-FTS, GOMOS, HALOE, HIRDLS, IASI, MLS, OSIRIS, POAM, SAGE II, SBUV, SCIAMACHY, SMILES (JAXA and NICT), SMR, as well as with MkIV balloon profiles and Umkehr measurements. A better agreement with reference instruments than for the previous version, V5R_O3_220 (Laeng et al., 2013), was demonstrated. The high bias near the ozone vmr peak has been significantly reduced by the use of spectral information from MIPAS band A only, three times more microwindows and adjusted regularization. The peak of particularly poor vertical resolution at 35 km, present in the previous version, is eliminated in this version.

The agreement with satellite limb and solar occultation reference instruments that have a known small bias vs. ozone sondes data (ACE-FTS, GOMOS, MLS, OSIRIS, SAGE II) is within 7 % in the lower and middle stratosphere (20–40 km) and 5 % in the upper troposphere. Around the ozone vmr peak, the agreement with most of satellite

reference instruments is within 5 %; this bias is as low as 3 % for ACE-FTS, MLS, OSIRIS, POAM and SBUV.

The agreement with HIRDLS, POAM and SCIAMACHY, is typically within 7 % in the lower and middle stratosphere and 10 % in the upper troposphere. In the lower meso-sphere, the best agreement (up to 22 %) is observed with GOMOS and SCIAMACHY. Near the ozone vmr peak, the agreement with ACE-FTS, MLS and OSIRIS is often less than about 3 %. The bias with respect to ACE-FTS for 15–45 km is less than 3 %. Good agreement with three MkIV balloon profiles is observed. The known high bias of Umkehr data is confirmed, the agreement of monthly means is within 20 % for 32–16 hPa and within 10 % for the other altitude layers provided by Umkehr data.

Overall, this MIPAS dataset has a small bias with respect to standard small-biased data records and can be used for climatological studies.

References

Adams, C., Bourassa, A. E., Bathgate, A. F., McLinden, C. A., Lloyd, N. D., Roth, C. Z., Llewellyn, E. J., Zawodny, J. M., Flittner, D. E., Manney, G. L., Daffer, W. H., and Degenstein, D. A.: Characterization of Odin-OSIRIS ozone profiles with the SAGE II dataset, Atmos. Meas. Tech., 6, 1447–1459, doi:10.5194/amt-6-1447-2013, 2013. 3979

Carlotti, M., Dinelli, B. M., Raspollini, P., and Ridolfi, M.: Geo-fit approach to the analysis of limb-scanning satellite measurements, Appl. Optics, 40, 1872–1885, 2001. 3956

Carlotti, M., Brizzi, G., Papandrea, E., Prevedelli, M., Ridolfi, M., Dinelli, B. M., and Magnani, L.: GMTR: Two-dimensional geo-fit multitarget retrieval model for Michelson Interferometer for Passive Atmospheric Sounding/Environmental Satellite observations, Appl. Optics, 45, 716–727, 2006. 3956

Damadeo, R. P., Zawodny, J. M., Thomason, L. W., and Iyer, N.: SAGE version 7.0 algorithm: application to SAGE II, Atmos. Meas. Tech., 6, 3539–3561, doi:10.5194/amt-6-3539-2013, 2013. 3979

Dufour, G., Eremenko, M., Griesfeller, A., Barret, B., LeFlochmoën, E., Clerbaux, C., Hadji-Lazaro, J., Coheur, P.-F., and Hurtmans, D.: Validation of three different scientific ozone products retrieved from IASI spectra using ozonesondes, Atmos. Meas. Tech., 5, 611–630, doi:10.5194/amt-5-611-2012, 2012. 3964, 3979

Dupuy, E., Walker, K. A., Kar, J., Boone, C. D., McElroy, C. T., Bernath, P. F., Drummond, J. R., Skelton, R., McLeod, S. D., Hughes, R. C., Nowlan, C. R., Dufour, D. G., Zou, J., Nichitiu, F., Strong, K., Baron, P., Bevilacqua, R. M., Blumenstock, T., Bodeker, G. E., Borsdorff, T., Bourassa, A. E., Bovensmann, H., Boyd, I. S., Bracher, A., Brogniez, C., Burrows, J. P., Catoire, V., Ceccherini, S., Chabrillat, S., Christensen, T., Coffey, M. T., Cortesi, U., Davies, J., De Clercq, C., Degenstein, D. A., De Mazière, M., Demoulin, P., Dodion, J., Firanski, B., Fischer, H., Forbes, G., Froidevaux, L., Fussen, D., Gerard, P., Godin-Beekmann, S., Goutail, F., Granville, J., Griffith, D., Haley, C. S., Hannigan, J. W., Höpfner, M., Jin, J. J., Jones, A., Jones, N. B., Jucks, K., Kagawa, A., Kasai, Y., Kerzenmacher, T. E., Kleinböhl, A., Klekociuk, A. R., Kramer, I., Küllmann, H., Kuttippurath, J., Kyrölä, E., Lambert, J.-C., Livesey, N. J., Llewellyn, E. J., Lloyd, N. D., Mahieu, E., Manney, G. L., Marshall, B. T., McConnell, J. C., McCormick, M. P., McDermid, I. S., McHugh, M., McLinden, C. A., Mellqvist, J., Mizutani, K., Murayama, Y., Murtagh, D. P., Oelhaf, H., Parrish, A., Petelina, S. V., Piccolo, C., Pommereau, J.-P., Randall, C. E., Robert, C., Roth, C., Schneider, M., Senten, C., Steck, T., Strandberg, A.,

Validation of MIPAS IMK/IAA V5R_O3_224 ozone profiles

A. Laeng et al.

Title Page

Abstract	Introduction
Conclusions	References
Tables	Figures

|◄ | ►|

◄ | ►

Back | Close

Full Screen / Esc

Printer-friendly Version

Interactive Discussion

Strawbridge, K. B., Sussmann, R., Swart, D. P. J., Tarasick, D. W., Taylor, J. R., Tétard, C., Thomason, L. W., Thompson, A. M., Tully, M. B., Urban, J., Vanhellemont, F., Vigouroux, C., von Clarmann, T., von der Gathen, P., von Savigny, C., Waters, J. W., Witte, J. C., Wolff, M., and Zawodny, J. M.: Validation of ozone measurements from the Atmospheric Chemistry Experiment (ACE), Atmos. Chem. Phys., 9, 287–343, doi:10.5194/acp-9-287-2009, 2009. 3979

Eckert, E., von Clarmann, T., Kiefer, M., Stiller, G. P., Lossow, S., Glatthor, N., Degenstein, D. A., Froidevaux, L., Godin-Beekmann, S., Leblanc, T., McDermid, S., Pastel, M., Steinbrecht, W., Swart, D. P. J., Walker, K. A., and Bernath, P. F.: Drift-corrected trends and periodic variations in MIPAS IMK/IAA ozone measurements, Atmos. Chem. Phys., 14, 2571–2589, doi:10.5194/acp-14-2571-2014, 2014. 3967

Froidevaux, L., Jiang, Y. B., Lambert, A., Livesey, N. J., Read, W. G., Waters, J. W., Browell, E. V., Avery, J. W. H. M. A., McGee, T. J., Twigg, L. W., Sumnicht, G. K., Jucks, K. W., Margitan, J. J., Sen, B., Stachnik, R. A., Toon, G. C., Bernath, P. F., Boone, C. D., Walker, K. A., Filipiak, M. J., Harwood, R. S., Fuller, R. A., Manney, G. L., Schwartz, M. J., Daffer, W. H., Drouin, B. J., Cofield, R. E., Cuddy, D. T., Jarnot, R. F., Knosp, B. W., Perun, V. S., Snyder, W. V., Stek, P. C., Thurstans, R. P., and Wagner, P. A.: Validation of Aura Microwave Limb Sounder stratospheric ozone measurements, J. Geophys. Res., 113, D15S20, doi:10.1029/2007JD008771, 2008. 3979

Glatthor, N., von Clarmann, T., Fischer, H., Funke, B., Gil-López, S., Grabowski, U., Höpfner, M., Kellmann, S., Linden, A., López-Puertas, M., Mengistu Tsidu, G., Milz, M., Steck, T., Stiller, G. P., and Wang, D.-Y.: Retrieval of stratospheric ozone profiles from MIPAS/ENVISAT limb emission spectra: a sensitivity study, Atmos. Chem. Phys., 6, 2767–2781, doi:10.5194/acp-6-2767-2006, 2006. 3957

Hubert, D., Verhoelst, T., Keppens, A., Granville, J., and Lambert, J.-C.: Network-Based Evaluation of Fourteen Satellite Limb/Occultation Profilers for the Next SPARC and WMO Ozone Trend Assessments, available at: http://larss.science.yorku.ca/QOS2012pdf/6028.pdf (last access: 14 April 2014), 2012. 3962

Hubert, D., et al.: Ground-based network assessment of fourteen occultation/limb ozone profilers over 1984–2012, Atmos. Chem. Phys. Discuss., in preparation, 2014. 3962

Imai, K., Fujiwara, M., Inai, Y., Manago, N., Suzuki, M., Sano, T., Mitsuda, C., Naito, Y., Hasebe, F., Koide, T., and Shiotani, M.: Comparison of ozone profiles between Superconducting Submillimeter-Wave Limb-Emission Sounder and worldwide ozonesonde measure-

Title Page

Abstract | Introduction

Conclusions | References

Tables | Figures

|◄ | ►|

◄ | ►

Back | Close

Full Screen / Esc

Printer-friendly Version

Interactive Discussion

ments, J. Geophys. Res.-Atmos., 118, 12755–12765, doi:10.1002/2013JD021094, 2013a. 3979

Imai, K., Manago, N., Mitsuda, C., Naito, Y., Nishimoto, E., Sakazaki, T., Fujiwara, M., Froidevaux, L., von Clarmann, T., Stiller, G. P., Murtagh, D. P., Rong, P.-P., Mlynczak, M. G., Walker, K. A., Kinnison, D. E., Akiyoshi, H., Nakamura, T., Miyasaka, T., Nishibori, T., Mizobuchi, S., Kikuchi, K.-I., Ozeki, H., Takahashi, C., Hayashi, H., Sano, T., Suzuki, M., Takayanagi, M., and Shiotani, M.: Validation of ozone data from the Superconducting Submillimeter-Wave Limb-Emission Sounder (SMILES), J. Geophys. Res.-Atmos., 118, 5750–5769, doi:10.1002/jgrd.50434, 2013b. 3979

Jégou, F., Urban, J., de La Noë, J., Ricaud, P., Le Flochmoën, E., Murtagh, D. P., Eriksson, P., Jones, A., Petelina, S., Llewellyn, E. J., Lloyd, N. D., Haley, C., Lumpe, J., Randall, C., Bevilacqua, R. M., Catoire, V., Huret, N., Berthet, G., Renard, J. B., Strong, K., Davies, J., Mc Elroy, C. T., Goutail, F., and Pommereau, J. P.: Technical Note: Validation of Odin/SMR limb observations of ozone, comparisons with OSIRIS, POAM III, groundbased and balloon-borne instruments, Atmos. Chem. Phys., 8, 3385–3409, doi:10.5194/acp-8-3385-2008, 2008. 3979

Jones, A., Murtagh, D., Urban, J., Eriksson, P., and Rösevall, J.: Intercomparison of Odin/SMR ozone measurements with MIPAS and balloonsonde data, Can. J. Phys., 85, 1111–1123, doi:10.1139/P07-118, 2007. 3979

Kasai, Y., Sagawa, H., Kreyling, D., Dupuy, E., Baron, P., Mendrok, J., Suzuki, K., Sato, T. O., Nishibori, T., Mizobuchi, S., Kikuchi, K., Manabe, T., Ozeki, H., Sugita, T., Fujiwara, M., Irimajiri, Y., Walker, K. A., Bernath, P. F., Boone, C., Stiller, G., von Clarmann, T., Orphal, J., Urban, J., Murtagh, D., Llewellyn, E. J., Degenstein, D., Bourassa, A. E., Lloyd, N. D., Froidevaux, L., Birk, M., Wagner, G., Schreier, F., Xu, J., Vogt, P., Trautmann, T., and Yasui, M.: Validation of stratospheric and mesospheric ozone observed by SMILES from International Space Station, Atmos. Meas. Tech., 6, 2311–2338, doi:10.5194/amt-6-2311-2013, 2013. 3979

Keim, C., Eremenko, M., Orphal, J., Dufour, G., Flaud, J.-M., Höpfner, M., Boynard, A., Clerbaux, C., Payan, S., Coheur, P.-F., Hurtmans, D., Claude, H., Dier, H., Johnson, B., Kelder, H., Kivi, R., Koide, T., López Bartolomé, M., Lambkin, K., Moore, D., Schmidlin, F. J., and Stübi, R.: Tropospheric ozone from IASI: comparison of different inversion algorithms and validation with ozone sondes in the northern middle latitudes, Atmos. Chem. Phys., 9, 9329–9347, doi:10.5194/acp-9-9329-2009, 2009. 3964

Kramarova, N. A., Frith, S. M., Bhartia, P. K., McPeters, R. D., Taylor, S. L., Fisher, B. L., Labow, G. J., and DeLand, M. T.: Validation of ozone monthly zonal mean profiles obtained from the version 8.6 Solar Backscatter Ultraviolet algorithm, Atmos. Chem. Phys., 13, 6887–6905, doi:10.5194/acp-13-6887-2013, 2013. 3968

5 Labow, G. J., McPeters, R. D., Bhartia, P. K., and Kramarova, N.: A comparison of 40 years of SBUV measurements of column ozone with data from the Dobson/Brewer network, J. Geophys. Res.-Atmos., 118, 7370–7378, doi:10.1002/jgrd.50503, 2013. 3979

Laeng, A. and Petropavlovskikh, I.: Comparison of MIPAS IMK/IAA Ozone with Umkehr Measurements, poster presented at 7th Atmospheric Limb Conference, 17–19 June 2013, Bremen, Germany, 2013. 3968, 3969

10 Laeng, A., Hubert, D., Verhoelst, T., von Clarmann, T., Dinelli, B. M., Dudhia, A., Raspollini, P., Stiller, G., Grabowski, U., Keppens, A., Kiefer, M., Sofieva, V., Froidevaux, L., Walker, K. A., Lambert, J.-C., and Zehner, C.: The Ozone Climate Change Initiative: comparison of four Level 2 Processors for the Michelson Interferometer for Passive Atmospheric Sounding (MI-15 PAS), Remote Sens. Environ., submitted, 2013. 3955, 3956, 3957, 3958, 3959, 3960, 3962, 3963, 3965, 3970, 3979, 3981

Mieruch, S., Weber, M., von Savigny, C., Rozanov, A., Bovensmann, H., Burrows, J. P., Bernath, P. F., Boone, C. D., Froidevaux, L., Gordley, L. L., Mlynczak, M. G., Russell III, J. M., Thomason, L. W., Walker, K. A., and Zawodny, J. M.: Global and long-term comparison of 20 SCIAMACHY limb ozone profiles with correlative satellite data (2002–2008), Atmos. Meas. Tech., 5, 771–788, doi:10.5194/amt-5-771-2012, 2012. 3979

Morris, G. A., Gleason, J. F., Russell III, J. M., Schoeberl, M. R., and McCormick, M. P.: A comparison of HALOE V19 with SAGE II V6.00 ozone observations using trajectory mapping, J. Geophys. Res., 107, ACH10.1–ACH10.9, doi:10.1029/2001JD000847, 2002. 3979

25 Nardi, B., Gille, J. C., Barnett, J. J., Randall, C. E., Harvey, V. L., Waterfall, A., Reburn, W. J., Leblanc, T., McGee, T. J., Twigg, L. W., Thompson, A. M., Godin-Beekmann, S., Bernath, P. F., Bojkov, B. R., Boone, C. D., Cavanaugh, C., Coffey, M. T., Craft, J., Craig, C., Dean, V., Eden, T. D., Francis, G., Froidevaux, L., Halvorson, C., Hannigan, J. W., Hepplewhite, C. L., Kinnison, D. E., Khosravi, R., Krinsky, C., Lambert, A., Lee, H., Loh, J., 30 Massie, S. T., McDermid, I. S., Packman, D., Torpy, B., Valverde-Canossa, J., Walker, K. A., Whiteman, D. N., Witte, J. C., and Young, G.: Initial validation of ozone measurements from the High Resolution Dynamics Limb Sounder, J. Geophys. Res.-Atmos., 113, D16S36, doi:10.1029/2007JD008837, 2008. 3979

Validation of MIPAS IMK/IAA V5R_O3_224 ozone profiles

A. Laeng et al.

Title Page	
Abstract	Introduction
Conclusions	References
Tables	Figures

◄◄	►►
◄	►
Back	Close

Full Screen / Esc

Printer-friendly Version

Interactive Discussion

Petropavlovskikh, I., Bhartia, P. K., and DeLuisi, J.: New Umkehr ozone profile retrieval algorithm optimized for climatological studies, Geophys. Res. Lett., 32, L16808, doi:10.1029/2005GL023323, 2005. 3968

Randall, C. E., Rusch, D. W., Bevilacqua, R. M., Hoppel, K. W., Lumpe, J. D., Shettle, E., Thompson, E., Deaver, L., Zawodny, J., Kyrö, E., Johnson, B., Kelder, H., Dorokhov, V. M., König-Langlo, G., and Gil, M.: Validation of POAM III ozone: comparisons with ozonesonde and satellite data, J. Geophys. Res., 108, 4367, doi:10.1029/2002JD002944, 2003. 3979

Raspollini, P., Carli, B., Carlotti, M., Ceccherini, S., Dehn, A., Dinelli, B. M., Dudhia, A., Flaud, J.-M., López-Puertas, M., Niro, F., Remedios, J. J., Ridolfi, M., Sembhi, H., Sgheri, L., and von Clarmann, T.: Ten years of MIPAS measurements with ESA Level 2 processor V6 – Part 1: Retrieval algorithm and diagnostics of the products, Atmos. Meas. Tech., 6, 2419–2439, doi:10.5194/amt-6-2419-2013, 2013. 3956

Sofieva, V. F., Rahpoe, N., Tamminen, J., Kyrölä, E., Kalakoski, N., Weber, M., Rozanov, A., von Savigny, C., Laeng, A., von Clarmann, T., Stiller, G., Lossow, S., Degenstein, D., Bourassa, A., Adams, C., Roth, C., Lloyd, N., Bernath, P., Hargreaves, R. J., Urban, J., Murtagh, D., Hauchecorne, A., Dalaudier, F., van Roozendael, M., Kalb, N., and Zehner, C.: Harmonized dataset of ozone profiles from satellite limb and occultation measurements, Earth Syst. Sci. Data, 5, 349–363, doi:10.5194/essd-5-349-2013, 2013. 3956, 3967

Tegtmeier, S., Hegglin, M. I., Anderson, J., Bourassa, A., Brohede, S., Degenstein, D., Froidevaux, L., Fuller, R., Funke, B., Gille, J., Jones, A., Krüger, Y. K. K., Kyrölä, E., Lingenfelser, G., Lumpe, J., Nardi, B., Neu, J., Pendlebury, D., Remsberg, E., Rozanov, A., Smith, L., Toohey, M., Urban, J., von Clarmann, T., Walker, K. A., and Wang, R. H. J.: SPARC Data Initiative: a comparison of ozone climatologies from international satellite limb sounders, J. Geophys. Res.-Atmos., 118, 12229–12247, doi:10.1002/2013JD019877, 2013. 3956, 3967

Toon, G. C.: The JPL MkIV Interferometer, Opt. Photonics News, 2, 19–21, 1991. 3969

van Gijsel, J. A. E., Swart, D. P. J., Baray, J.-L., Bencherif, H., Claude, H., Fehr, T., Godin-Beekmann, S., Hansen, G. H., Keckhut, P., Leblanc, T., McDermid, I. S., Meijer, Y. J., Nakane, H., Quel, E. J., Stebel, K., Steinbrecht, W., Strawbridge, K. B., Tatarov, B. I., and Wolfram, E. A.: GOMOS ozone profile validation using ground-based and balloon sonde measurements, Atmos. Chem. Phys., 10, 10473–10488, doi:10.5194/acp-10-10473-2010, 2010. 3979

Validation of MIPAS IMK/IAA V5R_O3_224 ozone profiles

A. Laeng et al.

Title Page

Abstract	Introduction
Conclusions	References
Tables	Figures

|◄ | ►|

◄ | ►

Back | Close

Full Screen / Esc

Printer-friendly Version

Interactive Discussion

von Clarmann, T.: Validation of remotely sensed profiles of atmospheric state variables: strategies and terminology, Atmos. Chem. Phys., 6, 4311–4320, doi:10.5194/acp-6-4311-2006, 2006. 3961

von Clarmann, T., Glatthor, N., Grabowski, U., Höpfner, M., Kellmann, S., Kiefer, M., Linden, A., Mengistu Tsidu, G., Milz, M., Steck, T., Stiller, G. P., Wang, D. Y., Fischer, H., Funke, B., Gil-López, S., and López-Puertas, M.: Retrieval of temperature and tangent altitude pointing from limb emission spectra recorded from space by the Michelson Interferometer for Passive Atmospheric Sounding (MIPAS), J. Geophys. Res., 108, 4736, doi:10.1029/2003JD003602, 2003. 3957

von Clarmann, T., Höpfner, M., Kellmann, S., Linden, A., Chauhan, S., Funke, B., Grabowski, U., Glatthor, N., Kiefer, M., Schieferdecker, T., Stiller, G. P., and Versick, S.: Retrieval of temperature, H_2O, O_3, HNO_3, CH_4, N_2O, $ClONO_2$ and ClO from MIPAS reduced resolution nominal mode limb emission measurements, Atmos. Meas. Tech., 2, 159–175, doi:10.5194/amt-2-159-2009, 2009. 3957

Wang, H. J., Cunnold, D. M., Thomason, L. W., Zawodny, J. M., and Bodeker, G. E.: Assessment of SAGE version 6.1 ozone data quality, J. Geophys. Res., 107, 4691, doi:10.1029/2002JD002418, 2002. 3979

Validation of MIPAS IMK/IAA V5R_O3_224 ozone profiles

A. Laeng et al.

Title Page

Abstract	Introduction
Conclusions	References
Tables	Figures

|◄ | ►|

◄ | ►

Back | Close

Full Screen / Esc

Printer-friendly Version

Interactive Discussion

Table 1. Microwindows used in the retrieval of V5R_O3_224 and V5R_O3_225.

Microwindows, cm^{-1}		6	9	12	15	18	21	24	27	30	33	36	39	42	45	48	51	54	57	60	63	66	69	72	75
687.6875	688.6875	-	-	-	-	-	-	-	-	-	T	-	T	T	T	T	T	T	T	T	T	T	T	T	T
689.3125	691.8750	-	-	-	-	-	-	T	T	T	-	-	T	T	T	T	T	T	T	T	T	T	T	T	T
692.2500	695.1875	-	-	-	-	-	-	-	-	-	T	T	T	T	T	T	T	T	T	T	T	T	T	T	T
707.1250	710.0625	-	-	-	-	-	-	-	T	T	T	T	T	T	T	T	T	T	T	T	T	T	T	T	T
712.3125	713.4375	T	T	T	-	-	-	-	-	-	-	T	T	T	T	-	T	-	-	-	-	-	T	T	T
713.5000	716.4375	T	T	T	-	-	-	T	T	T	-	T	T	T	T	T	T	-	T	T	T	T	T	T	T
716.5000	719.4375	-	T	-	-	-	-	T	T	-	T	T	T	T	T	T	T	T	T	T	T	T	T	T	T
720.7500	723.6875	-	-	T	-	-	-	T	T	T	T	T	T	T	T	T	T	T	T	T	T	T	T	T	T
728.5000	729.3750	T	T	-	-	-	-	-	-	-	T	T	T	T	T	T	T	T	T	T	T	T	T	T	T
730.0625	730.5000	-	T	T	-	-	-	-	-	-	T	T	T	T	T	T	T	T	T	T	T	T	T	T	T
731.9375	732.8750	T	T	-	-	-	T	T	T	-	-	T	-	-	-	T	T	T	T	T	-	T	T	-	T
734.0000	734.7500	T	T	-	-	-	-	-	-	-	T	T	-	T	T	T	T	T	-	-	-	-	T	T	T
736.4375	739.3750	T	T	-	-	T	T	-	T	-	T	T	T	T	T	T	T	T	T	T	T	T	T	T	T
739.4375	741.9375	T	T	-	-	-	-	-	T	T	T	T	T	T	T	T	T	T	T	T	T	T	T	T	T
745.2500	745.6875	T	-	T	T	T	-	-	-	-	T	T	T	T	T	T	T	T	T	T	T	T	T	T	T
746.6875	747.1250	T	T	-	T	-	T	T	T	T	T	T	T	T	T	T	T	T	T	T	T	T	T	T	T
747.6250	748.3750	T	-	-	-	-	-	T	T	T	T	-	T	T	T	T	T	T	-	-	T	T	T	T	T
749.5625	752.5000	T	-	-	T	-	T	T	T	-	T	T	T	T	T	T	T	T	T	T	T	T	T	T	T
752.9375	755.8750	-	-	-	-	T	T	T	-	-	T	T	T	T	T	T	T	T	T	T	T	T	T	T	T
758.3750	759.4375	-	-	-	T	T	T	T	T	T	T	T	T	T	T	T	T	T	T	T	T	T	T	T	T
759.5000	761.8750	T	T	T	T	-	-	T	-	-	T	T	T	T	T	T	T	T	T	T	T	T	T	T	T
765.0000	765.6250	T	T	T	T	-	-	-	-	-	-	T	T	T	T	T	T	T	T	T	T	T	T	T	T
767.5000	768.0000	-	T	T	T	T	T	T	T	T	T	T	T	T	T	T	T	T	T	T	T	T	T	T	T
771.8750	772.1250	T	-	T	T	T	T	T	T	T	T	T	T	T	-	-	T	T	T	T	T	T	T	T	T
774.2500	774.5625	T	-	-	T	-	T	T	T	-	-	T	-	T	T	T	-	-	T	-	-	T	T	-	-
776.5000	776.7500	T	-	-	-	-	-	-	-	-	-	-	T	T	-	T	-	T	T	T	T	T	-	-	-
780.2500	781.9375	T	T	T	T	T	-	-	-	-	T	T	T	T	T	T	T	T	T	T	T	T	T	T	T
788.9375	789.6875	T	T	T	T	-	-	-	-	T	T	T	T	T	T	T	T	T	T	T	T	T	T	T	T
790.7500	791.0000	T	-	T	T	T	-	-	-	-	-	-	-	-	-	-	T	-	-	-	-	-	-	-	-
791.1875	791.5625	T	T	T	-	T	T	-	-	-	-	T	T	T	T	T	T	T	T	T	T	T	T	T	T
1029.0000	1031.0000	-	-	-	-	-	-	-	-	-	-	-	-	-	-	-	T	T	T	T	T	T	T	T	T
1038.0000	1039.0000	-	-	-	-	-	-	-	-	-	-	-	-	-	-	-	T	T	T	T	T	T	T	T	T

Title Page

Abstract | Introduction

Conclusions | References

Tables | Figures

|◄ | ►|

◄ | ►

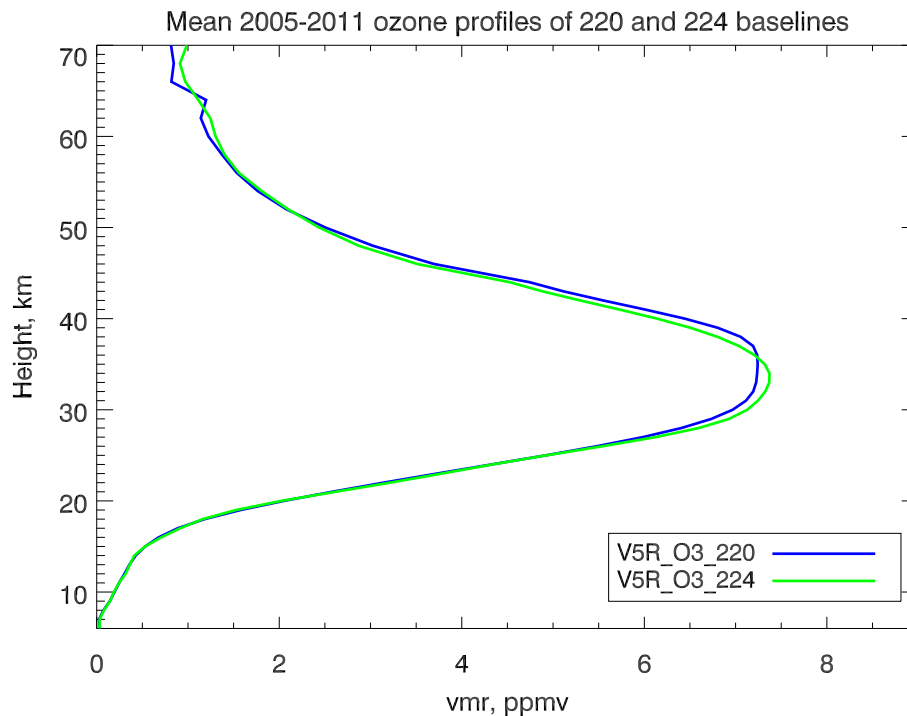Back | Close

Full Screen / Esc

Printer-friendly Version

Interactive Discussion

Table 2. Description of reference datasets.

Instrument	Version used in this study	Viewing geometry	Part of EM spectra	Time overlap	Collocation criteria	Number of matches	Description of what is provided as error	Latest validation and tropospheric bias wrt ozonesondes
MIPAS	V5R_O3_224, V5R_O3_225	limb emission	IR				measurement noise, randomly varying parameter errors	(Laeng et al., 2013)
ACE-FTS	v3.0	solar occultation	IR	Jan 2005–Sept 2010	5 h–500 km	5247	measurement noise only	(Dupuy et al., 2009), ±7 %
GOMOS	v6.0	stellar occultation	UV-VIS	2007–2009	5 h–500 km	21 351	measurement noise, scintillation correction error	(van Gijsel et al., 2010), ±3–5 % for dark limb
HALOE	v19	solar occultation	IR	Jan 2005–Aug 2005	5 h–500 km	164	measurement noise only	(Morris et al., 2002), 5–20 %[1]
HIRDLS	v7	limb emission	IR	Feb 2005–Mar 2008	5 h–500 km	80 121	measurement noise only	(Nardi et al., 2008), –10–20 %
IASI FORLI-O3		nadir	IR	16–23 Aug 2008	5 h–500 km	4162	measurement noise only	(Dufour et al., 2012), 10–25 %
MLS	v3.3	limb emission	MW	2005–2011	4 h–250 km	360 995	measurement noise, randomly varying parameter errors	(Froidevaux et al., 2008), 5 %
OSIRIS	v5.07	limb scatter	UV-VIS	2005–2011	5 h–500 km	143 450	measurement noise only	(Adams et al., 2013), ±5 %
POAM III	v4.0	solar occultation	UV-VIS	Jan 2005–Aug 2005	5 h–500 km	472	measurement noise, randomly varying parameter errors	(Randall et al., 2003), ±11 %
SAGE II	v7.0	solar occultation	VIS-NIR	Jan 2005–Aug 2005	5 h–500 km	189	measurement noise only	(Wang et al., 2002), 5 %, (Damadeo et al., 2013)
SBUV, NOAA 18	v8.6	nadir	UV	2005–2010	5 h–500 km	202 436	measurement noise only	(Labow et al., 2013)
SCIAMACHY	v2.5	limb scatter	UV-NIR	2008	5 h–500 km	151 539	measurement noise only	(Mieruch et al., 2012), ±10 %
SMILES JAXA	v2.1	limb emission	MW	Oct 2009–Apr 2010	5 h–500 km	17 262	measurement noise only	(Imai et al., 2013b, a), 5–7 %
SMILES NICT	v2.1.5	limb emission	MW	Oct 2009–Apr 2010	5 h–500 km	10 185	measurement noise only	(Kasai et al., 2013), ±8 %
SMR	v2.1	limb emission	MW	2005–2011	5 h–500 km	168 486	measurement noise only	(Jones et al., 2007; Jégou et al., 2008), ±10 %
MkIV balloon		solar occultation	IR	3 flights	24 h–1000 km	3	error estimate inferred from the fit residuals	
Umkehr ground based		zenith sky scatter	UV	2005–2012	24 h–1000 km	932	measurement noise, vertical smoothing	

Fig. 1. Mean ozone profiles of versions V5R_O3_220 and V5R_O3_224.
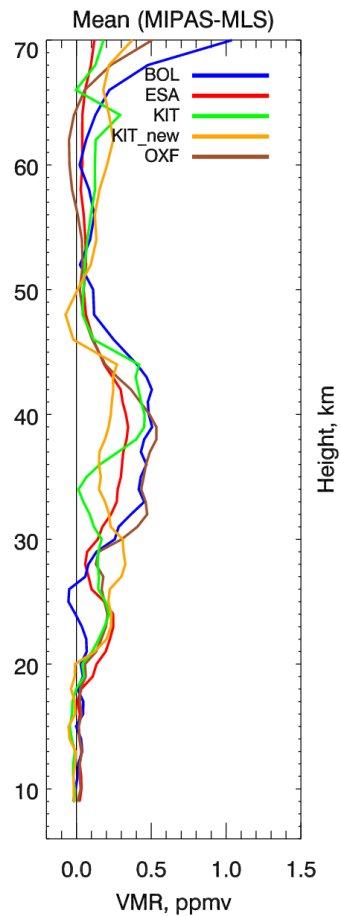
Fig. 2. Bias assessment of four MIPAS processors with respect to MLS from (Laeng et al., 2013) with bias of V5R_O3_224 overplotted (orange curve).
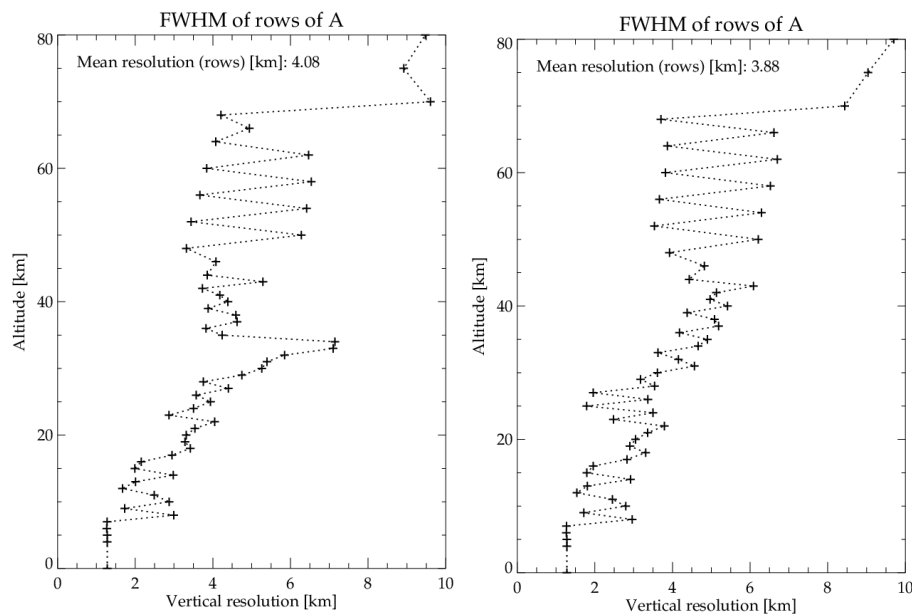
Fig. 3. Vertical resolution of MIPAS ozone profile on geolocation 20050219T181646Z for the versions V5R_O3_220 (left panel) and V5R_O3_224 (right panel).

Title Page

Abstract | Introduction

Conclusions | References

Tables | Figures

|◄ | ►|

◄ | ►

Back | Close

Full Screen / Esc

Printer-friendly Version

Interactive Discussion
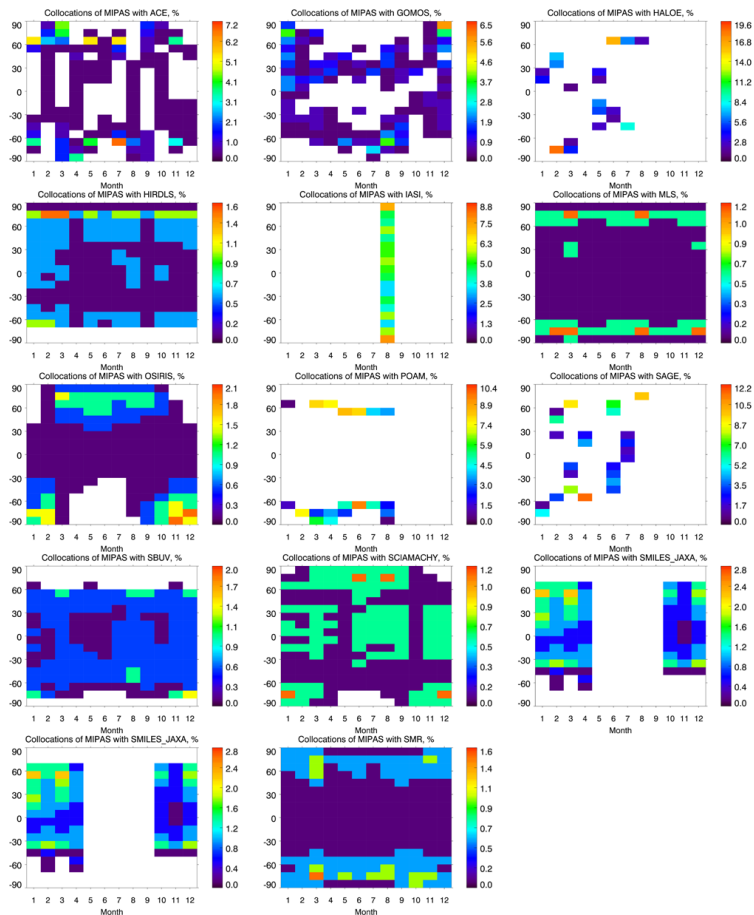
Fig. 4. Latitudinal distributions of collocated measurements of MIPAS with reference instruments, in percents. Note that the color scales are different on each panel.
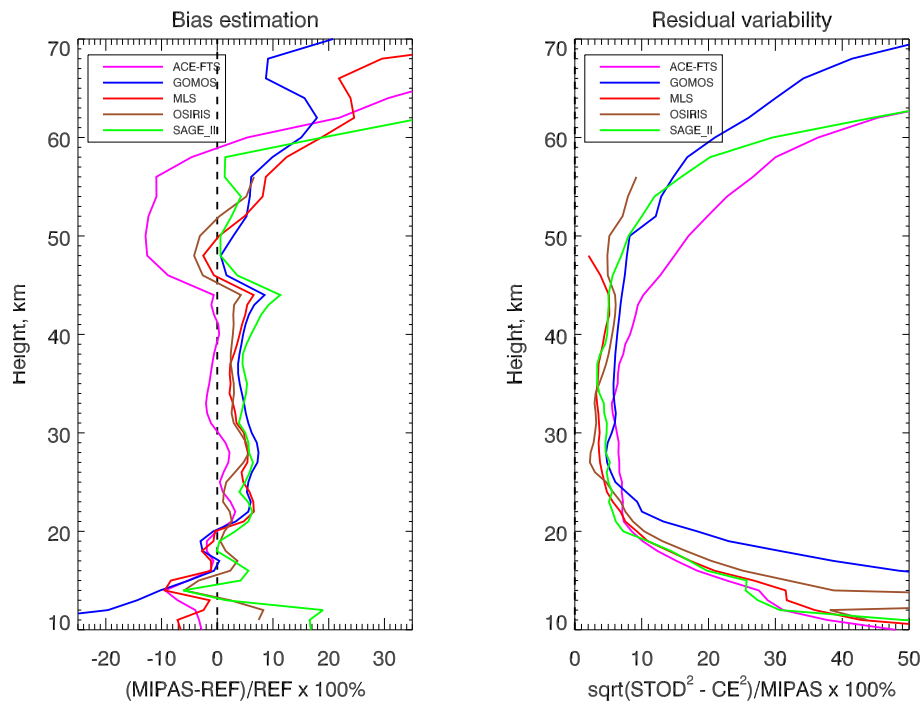
Fig. 5. Biases estimation and residual variability (Eq. 6) of MIPAS ozone profiles with respect to reference instruments that are small-biased compared to ozonesondes.
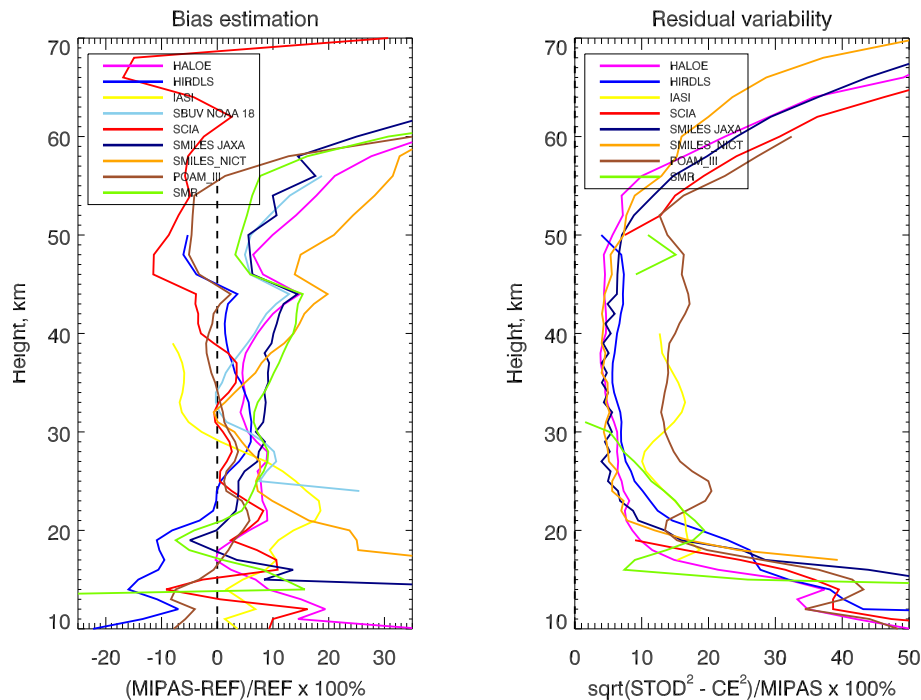
Fig. 6. Biases estimation and residual variability (Eq. 6) of MIPAS ozone profiles with respect to reference instruments that have known bias compared to ozonesondes. No bias correction has been applied.

Title Page

Abstract | Introduction

Conclusions | References

Tables | Figures

|◄ | ►|

◄ | ►

Back | Close

Full Screen / Esc

Printer-friendly Version

Interactive Discussion
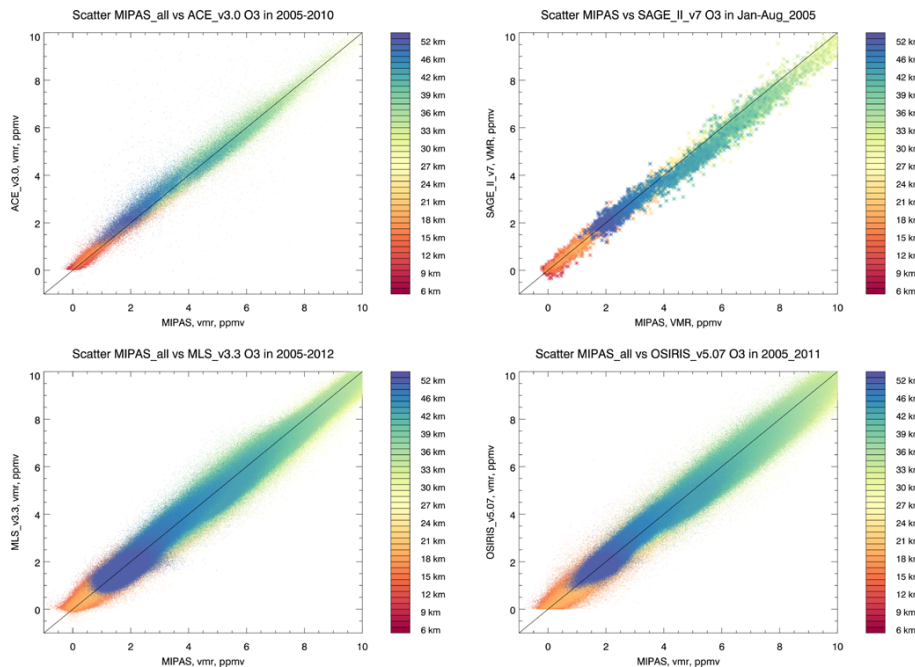
Fig. 7. Scatter plots of MIPAS ozone measurements with collocated measurements from small-biased solar occultation measurements (top panel) and small-biased limb measurements (bottom panel).
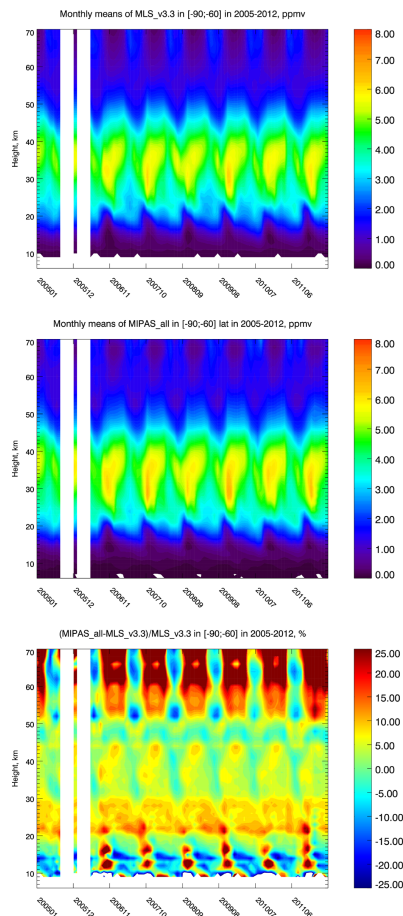
Fig. 8. Monthly mean ozone values (in ppmv) of MLS (top panel) and MIPAS (middle panel) and monthly means of relative differences MIPAS-MLS (bottom panel) in 2005–2011 at high southern latitudes.

Title Page

Abstract | Introduction

Conclusions | References

Tables | Figures

|◄ | ►|

◄ | ►

Back | Close

Full Screen / Esc

Printer-friendly Version

Interactive Discussion
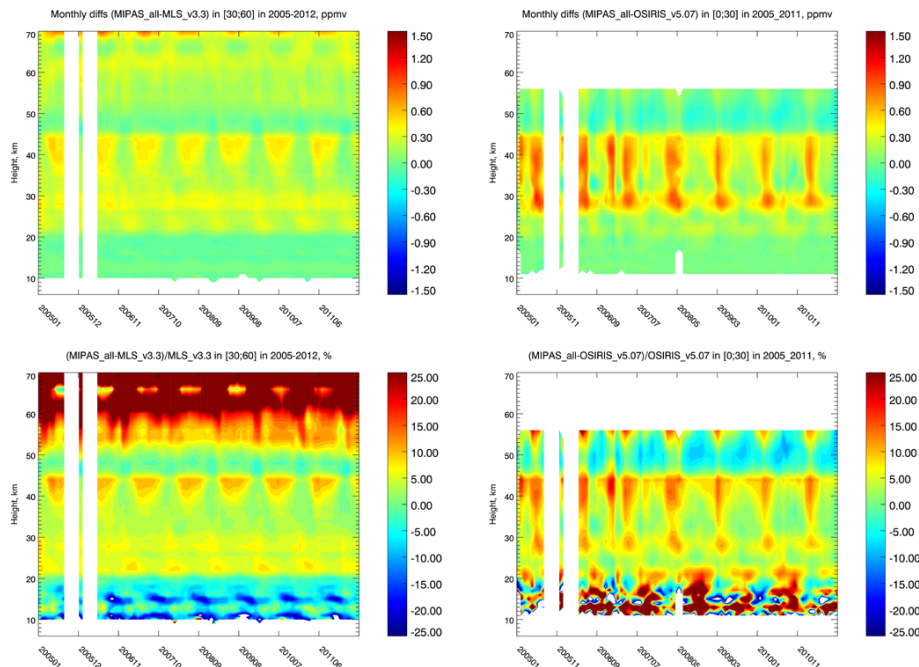
Fig. 9. Evolution of absolute (upper line) and relative (bottom line) differences between MIPAS and reference instrument in 2005–2012 on mid-northern latitudes for MLS (left column) and OSIRIS (right column).

Title Page

Abstract | Introduction

Conclusions | References

Tables | Figures

◀ | ▶

◀ | ▶

Back | Close

Full Screen / Esc

Printer-friendly Version

Interactive Discussion
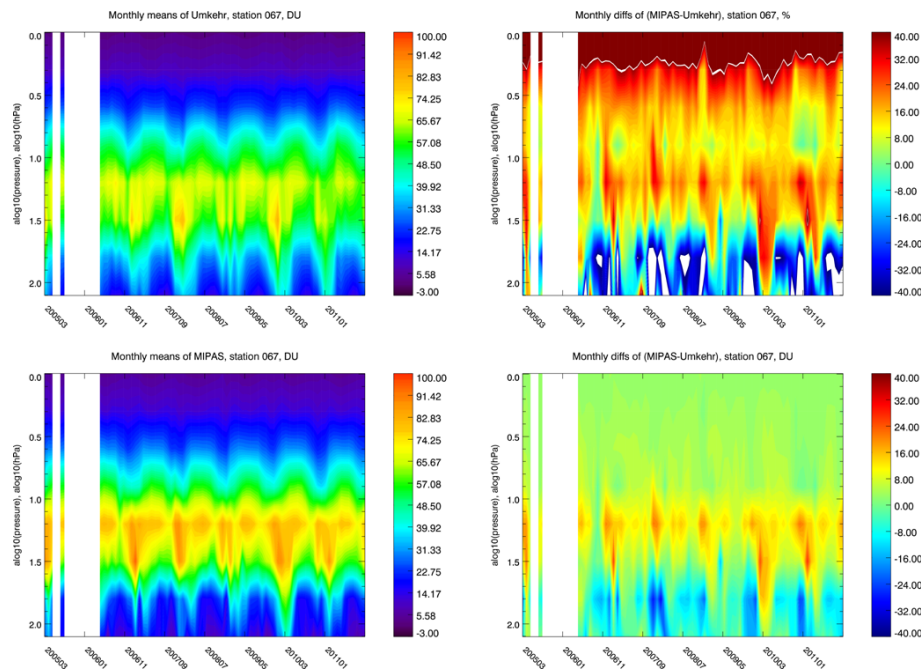
Fig. 10. Monthly mean ozone values (in DU) of Umkehr (top left panel) and MIPAS (bottom left panel) and monthly means of relative (top right panel) and absolute (bottom right panel) differences MIPAS-Umkehr in 2005–2012 at Boulder station, 40° N.
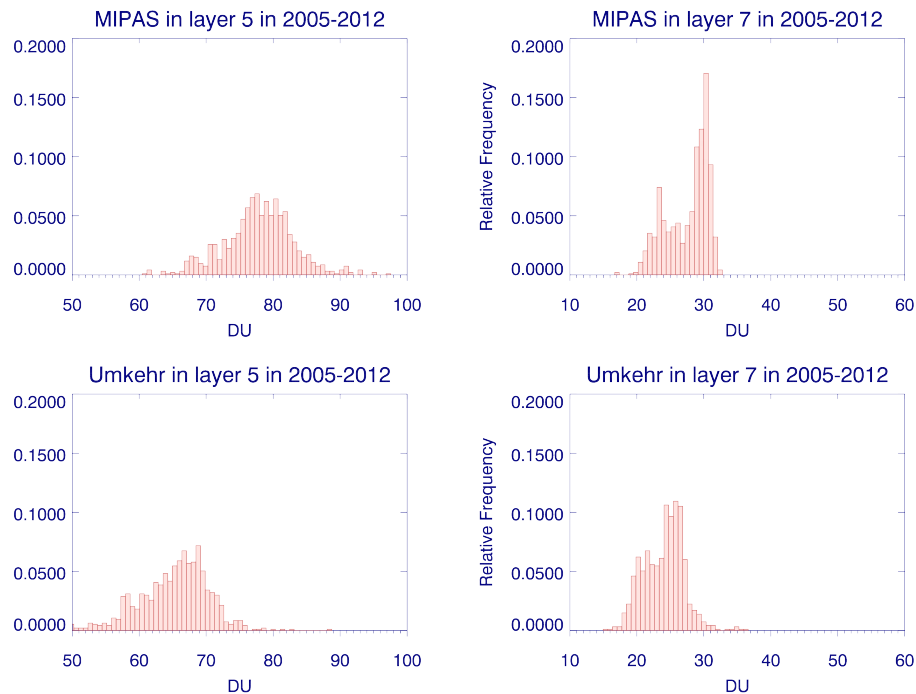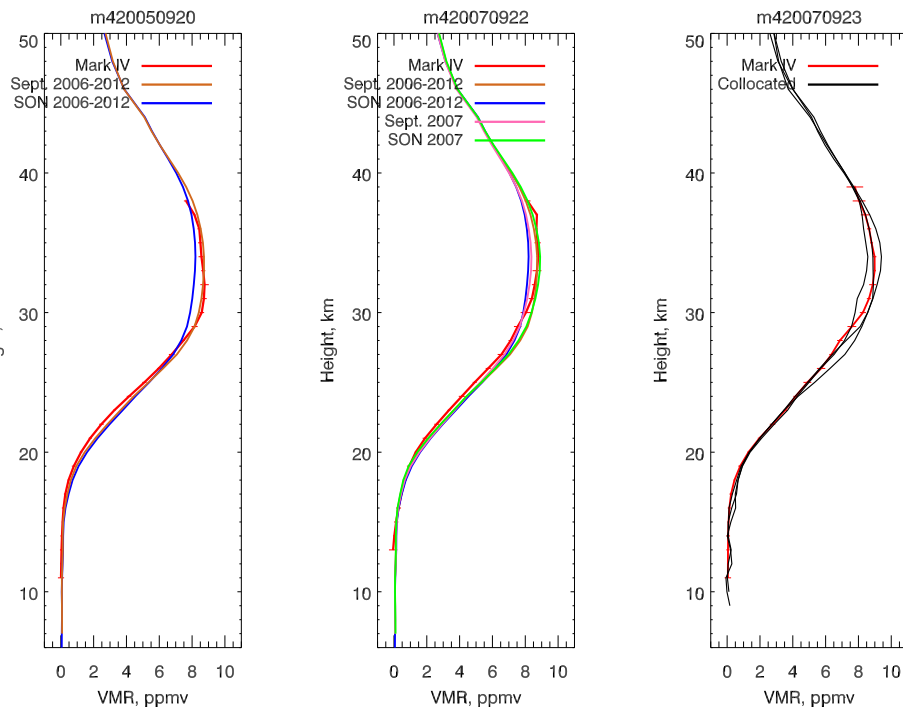
Fig. 11. Distribution of MIPAS (upper panels) and Umkehr (lower panels) O$_3$ values in layer 5 (left panels) and layer 7 (right panels) at Boulder station, 40° N. Layer 5 corresponds approximatively to 1.5–1.2 on *y* axis, and layer 7 to approximatively 0.9–0.5 on *y* axis.

Fig. 12. MkIV profiles and MIPAS O_3 vmr vertical profiles – collocated, monthly and seasonal means in corresponding latitude bands. All the means are taken in [30° N, 40° N] latitude band where the three balloon flights took place.

Title Page

Abstract | Introduction

Conclusions | References

Tables | Figures

|◄ | ►|

◄ | ►

Back | Close

Full Screen / Esc

Printer-friendly Version

Interactive Discussion